

General comparison of the surface processes involved in nitridation of Si(100)-2×1 by NH₃ and in SiN_x film deposition: A photoemission study

L. Kubler, J. L. Bischoff, and D. Bolmont

Faculté des Sciences et Techniques, Université de Haute Alsace, 4 rue des Frères Lumière, 68093-Mulhouse Cédex, France

(Received 13 May 1988)

With use of x-ray photoelectron spectroscopy (XPS), the adsorption of NH₃, both on *c*-Si(100) and during silicon nitride film growth, is comparatively examined over a wide range of substrate temperature T_S between room temperature and 800°C, gas pressure $P(\text{NH}_3)$, and exposure E . For sake of comparison with the surface parameters, dynamical exposure E_D or exposure times t_D are defined for the growth process. Both in surface adsorption and during film growth strongly correlated behaviors can be observed. They concern the following: (i) the general T_S -dependent evolution of the chemisorbed species, i.e., NH_x, H, and finally N, and (ii) the particular exposure and T_S behaviors of the latter nitridation regime, occurring in the 350–800°C range. At high T_S (600–800°C) and low NH₃ pressure, growth of Si₃N₄ islands on the *c*-Si(100) surface is related to heterogeneous SiN_x-film formation presenting strong phase separation (Si and Si₃N₄ cluster mixture). Very low nitrogen uptake, governed by N thermal desorption increasing with T_S , is found in this domain. For higher NH₃ pressures or exposures (E_D or $E > 200$ L, where L denotes langmuirs; 1 L = 10⁻⁶ Torr s) complete nitridation in thick Si₃N₄ films when Si is deposited or in a thin homogeneous Si₃N₄ overlayer on the *c*-Si surface, is achieved. At lower T_S (350–600°C) the nitrogen is chemisorbed at the surface in a more homogeneous way, the deficient bulk diffusion limiting interaction with the top layer and leading to a more rapid saturation of the nitrogen uptake with exposure. In this regime intermediate silicon subnitride environments Si-N₃Si are essentially found, whose counterpart for film deposition is nitride formation with a microstructure nearer to the random bonding model. Despite a T_S shift, due to the room-temperature dissociative chemisorption of O₂ on Si (while for atomic nitrogen it starts only above 350°C), we note a qualitative similarity between the main features involved in the initial, fast silicon nitridation stage and those occurring during oxidation.

I. INTRODUCTION

In semiconductor technology ammonia is the gas commonly used for many nitridation processes, e.g., high-temperature ($T > 1000$ K) chemical-vapor deposition (CVD), nitride layer growth by thermal nitridation, and low-temperature plasma deposition of silicon nitride films, hydrogenated or not (SiN_x:H or SiN_x). In spite of this considerable interest, in comparison with silicon oxidation, the mechanism of Si nitridation is not well understood over a range of substrate temperature (T_S), gas pressure $P(\text{NH}_3)$, or exposure (E) sufficiently large to obtain a general insight into the fundamental interactions between NH₃ and the Si surface in well-controlled ultrahigh vacuum (UHV) conditions.

Some Auger¹ or (XPS) x-ray photoelectron spectroscopy (Refs. 2 and 3) surface studies are mainly devoted to reactions at high T_S , and focus on the high-exposure domain ($E > 200$ L) (1 L = 10⁻⁶ Torr sec) relative to the slow thermal nitridation stage. Other low-energy electron diffraction (LEED),⁴ electron energy-loss spectroscopy (EELS),^{5,6} ultraviolet photoemission spectroscopy (UPS),⁷ or scanning tunneling microscopy⁸ (STM) reports are limited to restricted T_S or exposure ranges. The purpose of this work is to gain a better understanding of the Si-NH₃ system by surface adsorption (i) and film growth studies (ii) in similar large T_S or NH₃ pressure ranges, in

conjunction with comparisons between both experiments (iii).

(i) Using mainly XPS we investigate the thermal interaction of nondissociated NH₃ molecules upon clean Si(100)-2×1 surfaces in a T_S domain expanding from the room temperature (RT) to 800°C. By adjusting the exposure times, we are able to study, not only the slow nitridation stage at high exposures (already studied by other authors¹⁻³), but also the initial fast stage ($E < 200$ L) (Fig. 1). We especially focus on this latter range, which is not well studied and, as we will show, appears particularly useful for comparisons with the film-growth processes. Furthermore the slow stage time dependence (at constant pressure) and pressure dependence (at constant time) of the nitridation rate are determined with greater precision.

(ii) We also report, as a function of the same parameters, the nitrogen uptake during SiN_x or SiN_x:H film growth by reactive evaporation of Si under an NH₃ ambient. This method is suitable to study the T_S -dependent introduction of species only issuing from the Si surface reactivity with molecular NH₃ and not with other dissociated fragments (NH or NH₂) as it occurs with plasma-aided methods.

(iii) In order to compare the exposure data on *c*-Si surfaces and the kinetics of nitrogen incorporation during film growth, we define a dynamical exposure E_D [ex-

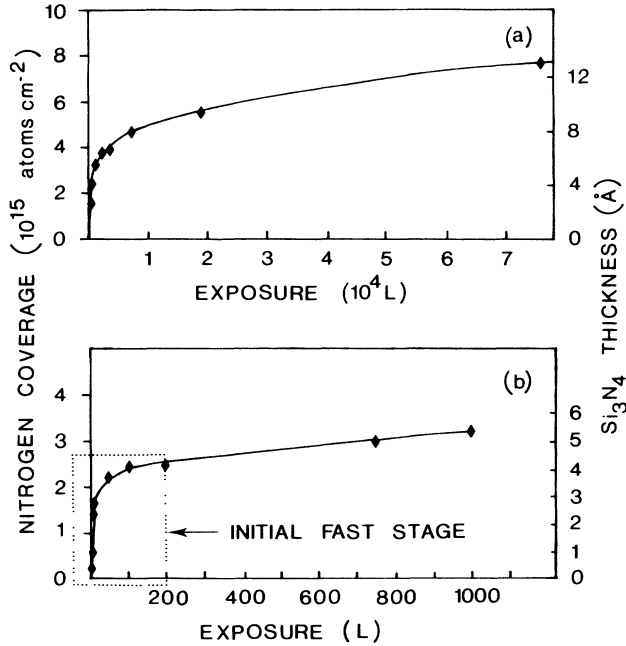


FIG. 1. Nitrogen uptake (using XPS), expressed in atoms cm^{-2} (left scale) or in silicon nitride thickness (right scale) as a function of exposure at constant NH_3 pressure (10^{-5} mbar), T_S (700°C), and varying times. Note the strong exposure scale change between the initial fast nitridation (lower curve) and the slow and saturating one (upper curve).

pressed in langmuirs (L)], with respect to the relevant NH_3 deposition pressure (in Torr) as follows:

$$E_D \text{ (L)} = 10^6 P(\text{NH}_3) t_D = 10^6 P(\text{NH}_3) \frac{d}{r},$$

where the ratio d/r between the mean interlayer distance (d) and the evaporation rate (r) represents a mean exposure time t_D for the growing film overlayer. In this way we show that initial dynamical exposures E_D between 0 and 200 L are sufficient to produce the whole range of possible nitride compounds SiN_x where x is between 0 and 1.33. The importance of the knowledge of the initial nitridation stage, accessible only by UHV studies, is thus emphasized. However, many other interesting features can be deduced from the combined observation of the nitrogen adsorption curves and the nitrogen incorporation during SiN_x film formation, particularly the general similarity of the successive nitridation regimes found in both cases as a function of rising T_S such as dissociative coadsorption above RT of NH_2 or NH species with hydrogen, followed by progressive desorption, first of the NH_x fragments, and then by H, allowing the rapid start of the thermal nitridation above 350°C . This low- T_S NH_x adsorption regime that we were the first to establish, essentially by UPS studies, is detailed in our previous reports for film growth^{9,10} as well as for adsorption on $c\text{-Si}(111)\text{-}7\times 7$ (Ref. 11) and $c\text{-Si}(100)\text{-}2\times 1$ (Ref. 12) surfaces and has also been confirmed by another study.¹³

The high- T_S regime provides the newest and most important topics of this paper: below 600°C essentially sub-nitride Si environments are formed regardless of the pressure. Between 600 and 800°C a much stronger phase separation is found, via enhanced nitrogen diffusion and desorption, leading to a heterogeneous Si_3N_4 island growth (at least for low exposures) on the $c\text{-Si}$ surface, and a correlated formation of a $\text{Si-Si}_3\text{N}_4$ cluster mixture for the deposited films. The control of the cluster formation on a microscopic scale, is a general and very important problem in the preparation of binary amorphous alloys. In fact, their electronic properties are often determined by this microstructure. It is interesting to note such correlations between surface phase segregation and cluster formation in deposited films in the same exposure and T_S range. In general this work should be understood as an attempt to gain better comprehension for binary film growth, illustrated by the example of the silicon nitride system, by the means of better knowledge of the surface adsorption mechanisms at the Si-gas interface.

II. EXPERIMENT

All XPS analyses or film depositions were performed in the same UHV chamber whose base pressure was in the 10^{-10} -mbar range. The photoelectron spectra were recorded with a VG-CLAM 100 spectrometer operating with a $\text{Mg } K\alpha$ x-ray (1253.6-eV) source. The substrates were nearly intrinsic, p -type $10\text{-}\Omega\text{ cm}$ $c\text{-Si}(100)$ wafers whose temperature T_S could be varied by direct Joule heating between RT and 800°C and measured with a Chromel-Alumel thermocouple. Clean $c\text{-Si}(100)\text{-}2\times 1$ reconstructed surfaces, characterized by the well-known UPS surface-state signature, were generated by repeated cycles of Ar^+ sputtering and annealing at 800°C . A range of controlled exposures, determined by noncorrected gauge readings, is provided by introduction of NH_3 (99.995% purity) into the chamber via a leak valve during controlled times, followed by rapid pumping. The nitride films were deposited by electron beam evaporation of Si under controlled NH_3 pressures ($10^{-6}\text{-}10^{-4}$ mb), the Si impinging rate (r_{Si}) being kept constant at ~ 0.8 \AA sec^{-1} . This allows one to obtain nearly constant dynamical exposure times t_D for the growing surface and dynamical exposures E_D , determined by the working NH_3 pressure, comparable to the exposures used for the Si surface adsorption. Nevertheless the constancy of t_D is only true at first approximation, considering the T_S -dependent nitrogen uptake which modifies the evaporation rate. That is why, when T_S varies, we do not work strictly at constant E_D even if silicon evaporates at constant NH_3 pressure and Si impinging rates. For instance, in Fig. 3 we indicate the varying E_D values taking in account the true evaporation rate $r(\text{SiN}_x)$ deduced from $r(\text{Si})$ by

$$r(\text{SiN}_x) = r(\text{Si}) \frac{28 + 14x}{28}.$$

All reported binding energies (BE) are referred to the Fermi level. The nitrogen covering the $c\text{-Si}$ surface, or incorporated in the deposited films is generally derived

from doing N 1s and Si 2p signal intensity ratios, the instrumental effects being removed if the spectra are recorded in the same conditions (x-ray photon flux, analyzed areas, etc). The substrate holder could be rotated in order to change the emission angle θ relative to the surface normal. We generally used a large angle θ , which will enhance surface contribution, for quantitative adsorbate determinations. The smaller angles, sampling deeper in the bulk, were allowed to reach the atomic concentration in the bulk alloys (SiN_x) and to check the in-depth homogeneity of the elements.

A. Determination of the bulk concentration x

On the basis of a spatial uniformity the relative nitrogen concentration x was calculated as it follows:

$$x = \frac{N_N}{N_{\text{Si}}} \cdot \frac{I_N^\infty(\text{SiN}_x)}{I_{\text{Si}}^\infty(\text{SiN}_x)} = \frac{N_N}{N_{\text{Si}}} \frac{\alpha_N}{\alpha_{\text{Si}}} \frac{T_N}{T_{\text{Si}}} \frac{\lambda_N(\text{SiN}_x)}{\lambda_{\text{Si}}(\text{SiN}_x)},$$

where N_X is the atomic concentration of the element X , α the photoelectric cross section for the particular transition, T the spectrometer transmission factor, and λ the mean free path of the electrons in the sample with T and λ depending on the kinetic energy E_K of the electrons. I_X^∞ is the signal intensity considering a thickness layer $d \gg \lambda$. (For this purpose the thickness of our deposited SiN_x films is always $> 500 \text{ \AA}$.) We obtain

$$x = \frac{I_N^\infty(\text{SiN}_x)}{I_{\text{Si}}^\infty(\text{SiN}_x)} \frac{S_{\text{Si}}}{S_N},$$

where S_X , the atomic sensitivity factor of the element X , is given by $S = \alpha T \lambda$. The absolute determinations or the tabulated values in the literature for S are generally very imprecise. Therefore it is necessary to develop a relative calibration of S . The Si_3N_4 layer growth, by thermal nitridation, allows an improved precision if the analyses are performed *in situ*, the stoichiometry now being fixed in this case at $x = 1.33$ so that

$$\frac{S_{\text{Si}}}{S_N} = 1.33 \frac{I_{\text{Si}}^\infty(\text{Si}_3\text{N}_4)}{I_N^\infty(\text{Si}_3\text{N}_4)}.$$

Unfortunately the determination of $I_{\text{Si}}^\infty(\text{Si}_3\text{N}_4)/I_N^\infty(\text{Si}_3\text{N}_4)$ is not possible, the thermal nitridation, as shown below, being rapidly saturated and limited in thickness. Hence we only succeed experimentally to $I_{\text{Si}}^d(\text{Si}_3\text{N}_4)/I_N^d(\text{Si}_3\text{N}_4)$, where d is the nitride thickness on the *c*-Si substrate. But a simple calculation relates the two previous ratios:

$$\frac{I_{\text{Si}}^d(\text{Si}_3\text{N}_4)}{I_N^d(\text{Si}_3\text{N}_4)} = \frac{I_{\text{Si}}^\infty(\text{Si}_3\text{N}_4)}{I_N^\infty(\text{Si}_3\text{N}_4)} f(d),$$

where

$$f(d) = \frac{1 - \exp[-d/\lambda_{\text{Si}}(\text{Si}_3\text{N}_4)\cos\theta]}{1 - \exp[-d/\lambda_N(\text{Si}_3\text{N}_4)\cos\theta]}.$$

$f(d)$ is a weakly varying correcting factor in which the λ or d imprecision is not critical. Using the well-known square-root dependence of λ with kinetic energy E_K in the XPS domain

$$\frac{\lambda_N(\text{Si}_3\text{N}_4)}{\lambda_{\text{Si}}(\text{Si}_3\text{N}_4)} = \left(\frac{E_K(\text{N})}{E_K(\text{Si})} \right)^{1/2},$$

and taking $\lambda_{\text{Si}}(\text{Si}_3\text{N}_4) = 30 \text{ \AA}$,^{14,2} $f(d)$, at normal emission, has a value between 0.86 and 1 if d varies between 0 and ∞ . We find

$$x = \frac{S_{\text{Si}}}{S_N} \frac{I_N^\infty(\text{SiN}_x)}{I_{\text{Si}}^\infty(\text{SiN}_x)},$$

where

$$S_{\text{Si}}/S_N = 1.33 \frac{I_{\text{Si}}^d(\text{Si}_3\text{N}_4)}{I_N^d(\text{Si}_3\text{N}_4)} f(d).$$

B. Determination of high nitrogen coverage on *c*-Si surfaces

For the purpose of determining high nitrogen coverage on *c*-Si it is possible to work with the intensity ratios of N 1s and Si 2p in the nitride $I_{\text{Si}}^d(\text{Si}_3\text{N}_4)$ or in the substrate $I_{\text{Si}}^d(\text{Si})$ or only with the two Si 2p signals well resolved in BE by the changing charge state in pure Si and in the nitride. This latter case leads to

$$d = \lambda_{\text{Si}}(\text{Si}_3\text{N}_4)\cos\theta \ln \left[\frac{I_{\text{Si}}^d(\text{Si}_3\text{N}_4)/I_{\text{Si}}^d(\text{Si})}{I_{\text{Si}}^\infty(\text{Si}_3\text{N}_4)/I_{\text{Si}}^\infty(\text{Si})} + 1 \right],$$

$$\frac{I_{\text{Si}}^\infty(\text{Si}_3\text{N}_4)}{I_{\text{Si}}^\infty(\text{Si})} = \frac{N_{\text{Si}}(\text{Si}_3\text{N}_4)}{N_{\text{Si}}(\text{Si})} \frac{\lambda_{\text{Si}}(\text{Si}_3\text{N}_4)}{\lambda_{\text{Si}}(\text{Si})} = 1.16,$$

with $\lambda_{\text{Si}}(\text{Si}) = 23 \text{ \AA}$ (Ref. 15) and where $N_{\text{Si}}(\text{Si}_3\text{N}_4)/N_{\text{Si}}(\text{Si})$ is the ratio between the concentration or partial density of Si in the nitride (2.07 g/cm^3) and that of pure silicon (2.33 g/cm^3) and

$$d (\text{ \AA}) = 30 \cos\theta \ln \left[\frac{I_{\text{Si}}^d(\text{Si}_3\text{N}_4)(\theta)/I_{\text{Si}}^d(\text{Si})(\theta)}{1.16} + 1 \right].$$

The silicon nitride structure giving $5.89 \times 10^{22} \text{ atoms/cm}^3$ the thickness d can easily be converted in surface density Q_N of the nitrogen uptake. If the nitride layer is relatively small, a more sensitive way is to use

$$\frac{I_N^d(\text{Si}_3\text{N}_4)}{I_{\text{Si}}^d(\text{Si})}.$$

For the sake of brevity, we do not develop the similar formalism for the determination of d in this case.

C. Determination of low nitrogen coverage on *c*-Si surfaces

If the surface coverage becomes lower than a monolayer referred to a density of $6.8 \times 10^{14} \text{ atoms/cm}^2$, the (100) plane density at monolayer completion as occurs, for instance, for initial high- T_S nitridation or RT adsorption at all exposures, it is no longer possible to think in terms of nitride thickness; it is now necessary to determine a surface adsorbate concentration which must be sufficiently weak so that only negligible attenuation of the silicon substrate signal I_{Si}^∞ could be observed. On this basis we obtain the following relationship:

$$Q_N = \frac{I_N(\theta) S_{Si}}{I_{Si}^\infty(\theta) S_N} \left(\frac{E_K(N)}{E_K(Si)} \right)^{1/2} \lambda_{Si}(Si) N_0(Si) \cos\theta,$$

where $\lambda_{Si}(Si)$ equals mean free path of Si $2p$ electrons in Si (23 Å), $N_0(Si)$ equals bulk Si concentration which is equal to 5.0×10^{22} atoms/cm³, and Q_N equals the surface nitrogen concentration in atoms/cm². The Q_N values obtained by (B) or (C) calculations in their borderline cases fit well to each other.

III. RESULTS

Figure 1 illustrates the domain studied and the two different nitridation stages occurring at high T_S as a function of exposure:

(A) the initial fast step, arbitrarily limited at $E \sim 200$ L on which we will focus in Sec. III A.

(B) the much slower and saturating step at higher exposures is addressed in Sec. III B.

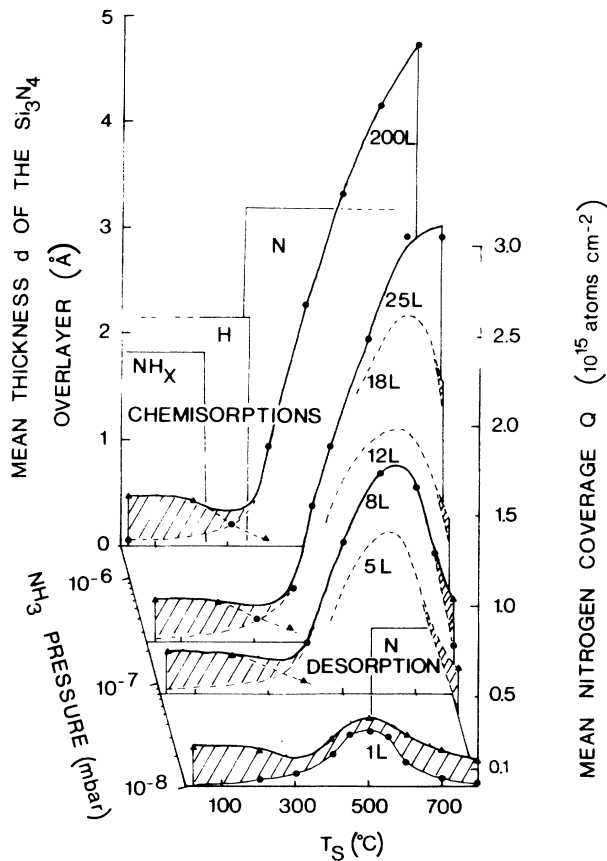


FIG. 2. Evolution of the nitrogen uptake (expressed in atoms cm⁻² or in silicon nitride mean thickness) upon *c*-Si(100) surfaces in the initial nitridation stage as a function of T_S or NH_3 pressure, at constant exposure times (133 sec). For the sake of clarity the entire curves for 5, 12, and 18 L are not represented. The dashed areas correspond to the contributing part of the low- T_S chemisorption (NH_x species) presenting higher N 1s BE's than the nitride contributions. The indicated Si_3N_4 thicknesses d are only sound for $T_S > 350^\circ C$ (high- T_S stage).

A. The initial fast-nitridation stage

For this first stage, the figures sum up the nitrogen uptake on *c*-Si(100) (Fig. 2) and during film growth (Fig. 3), over the entire T_S range and as a function of pressure or exposure (E for *c*-Si or E_D in case of film deposition) at constant exposure times (133 sec for *c*-Si). The generality of these data, of which some partial curve evolutions have been recently published,⁹⁻¹² reveals the similarity, as a function of T_S , between the main interaction processes involved in thermal nitridation of clean *c*-Si surfaces and during silicon nitride film growth. Two opposed nitridation behaviors on both sides of a nitrogen-uptake minimum, near $300^\circ C$, particularly marked in Fig. 3, are evidenced.

1. Low T_S regime

For T_S below $300^\circ C$ the nitridation decreases, while above $300^\circ C$ it increases with increasing T_S . The occurrence of two different N adsorption mechanisms is

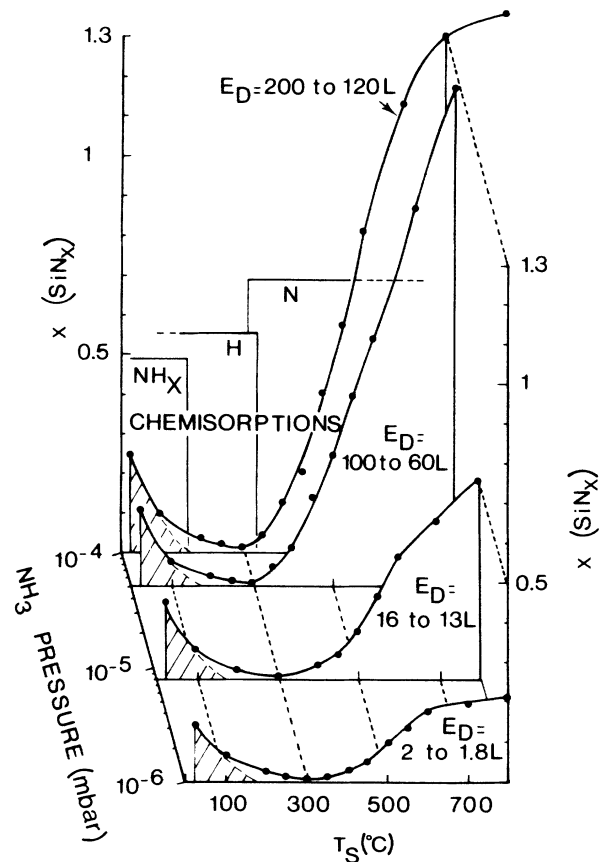


FIG. 3. Nitrogen bulk content x (in atomic concentration relative to silicon) deduced by XPS in deposited SiN_x or $SiN_x:H$ films as a function of T_S or NH_3 pressure the impinging Si flux being kept constant ($r_{Si} \sim 0.8$ Å/sec). As the nitrogen uptake, at constant NH_3 pressure, is varying with T_S , the indicated values of the dynamical exposures E_D are slightly variable for a given $P(NH_3)$.

further corroborated by the systematically higher BE of the N 1s core level (Figs. 4 and 5) for the low- T_S process [398.0 eV in films, 398.6 eV on *c*-Si(100)- 2×1 (line γ) at RT, compared to 397.4 eV above 300 °C (line β)]. Furthermore, some line asymmetries and broadenings prove the simultaneous presence of various local environments for the nitrogen. Such features are particularly well displayed by the N 1s signals at low exposures (Figs. 4 and 5), where no dominant β line masks the weaker γ line. Due to restricted space, the other sets of N 1s lines (at higher exposures) are not given. Using extended UPS investigations, in this low- T_S adsorption regime, we have previously^{11,12} established the adsorption of partially dissociated fragments NH_x (where $x=1$ or 2). In a more recent study¹⁶ we even suggested that the species mainly incorporated in the films ($E_B=398.0$ eV) would be due to $\text{Si}_2\text{—N—H}$ bonds, and that the adsorbed species on *c*-Si(100)- 2×1 surfaces would be understood as NH_2 fragments ($E_B=398.6$ eV). The sticking coefficient of this low- T_S NH_x -adsorption process must be very high, since the coverage decreases very slowly with decreasing exposures in the one-Langmuir range. We have to notice that such NH_x assignments for the RT adsorption of NH_3 on Si were recently supported by EELS studies.⁵ An increasing desorption or thermal dissociation of these NH_x

species can explain the general decreasing uptake when T_S increases. In this circumstance, the difference between the adsorbed species on *c*-Si(100) surface (NH_2) and during film growth (NH) can account for the more rapid decrease observed for the low- T_S adsorption regime (Figs. 3 and 5) in this latter case and, hence, the more pronounced minimum between the low- and high- T_S regimes. But other reasons more specific to the deposition process, such as the modification of the desorption regime during the film growth by electron-stimulated desorption (ESD) or by the impinging Si-atom flux, may also be invoked.

Near 300 °C, in the T_S region intersecting the low- and high- T_S regimes we are able to detect both in films¹⁶ or on the *c*-Si(100) surface,¹² UPS features attributed to Si—H bonds in the monohydride form. Thus, films grown in this T_S range, although appearing fully pure by XPS (no nitrogen uptake), do not present the rapid oxygen surface contamination characteristic of pure, amorphous Si. This silicon dangling-bond passivation also proves the presence of hydrogen. The H adsorption, a by-product of the dissociation of NH_3 to NH_x and H, is probably also present at RT but may be masked by the more prominent UPS features of the NH_x species until

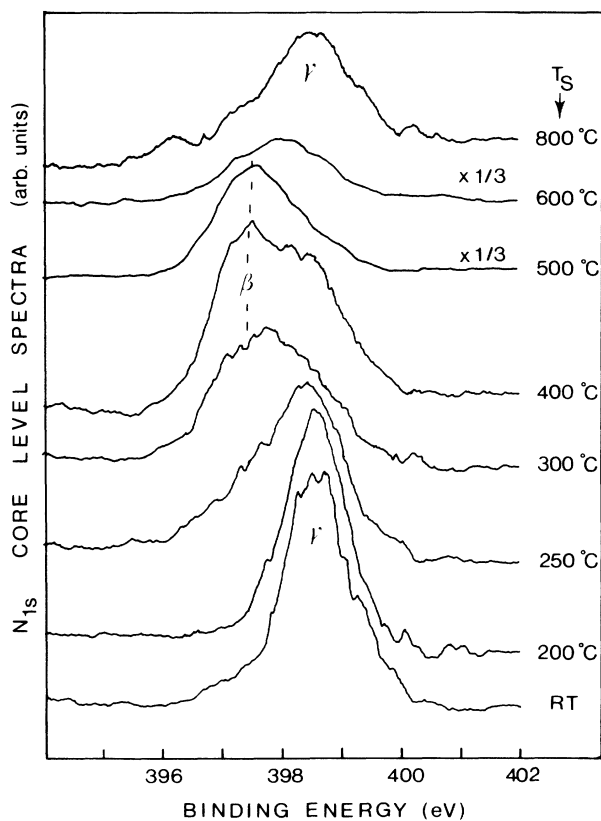


FIG. 4. Typical N 1s core-level spectra obtained after a 1-L exposure to NH_3 of *c*-Si(100)- 2×1 surfaces held at various T_S [$t=133$ sec, $P(\text{NH}_3)=10^{-8}$ mbar].

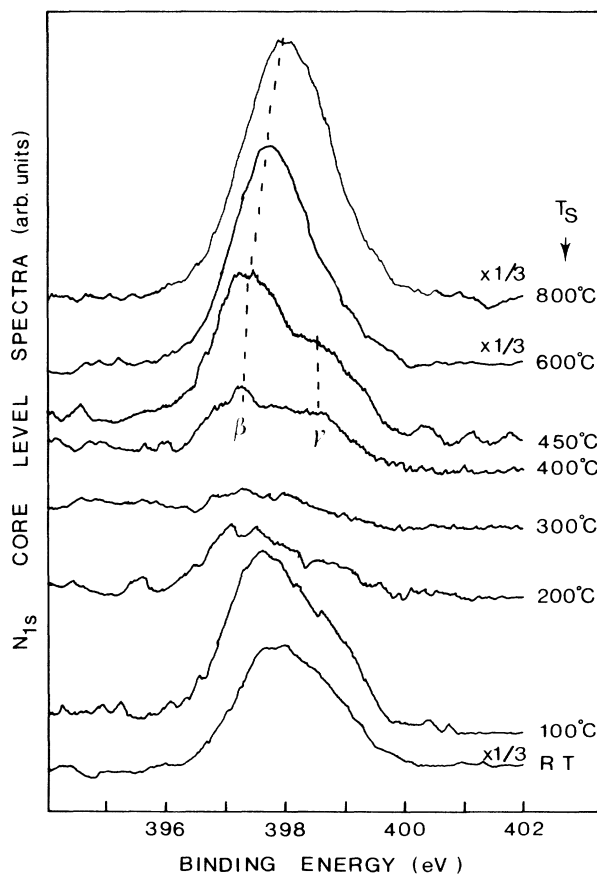


FIG. 5. Typical N 1s core-level spectra for nitrogen in nitride films, deposited at various T_S under nearly constant dynamical exposure [$r_{\text{Si}}\sim 0.8$ Å/sec, $P(\text{NH}_3)=10^{-6}$ mbar].

their desorption. Indeed the NH_x surface coverage after a RT saturation exposure of the Si(100) surface (0.25–0.30 ML) seems too low to account for the complete saturation of the dangling bonds. Besides nitrogen incorporation in the NH form during the film growth at RT saturates too, whatever the NH_3 pressure, at values slightly above $x \sim 0.20$ in these $\text{SiN}_x\text{:H}$ samples. Furthermore, the exposure or pressure-dependent behaviors are other typical features distinguishing the low- and high- T_S regimes. This brings us now to the central topic of this article, i.e., the true thermal nitridation which has not been well studied, at least during the first step of NH_3 adsorption.

2. High T_S regime

In contrast to the γ line which saturates very early with exposure, the line labeled β , with lower BE (~ 397.4 eV), increases with exposure and T_S above 350°C . This form of nitrogen is attributed to chemisorbed atomic species coming from completely dissociated NH_3 .^{10,11} These adatoms in a nitride environment N-Si₃ are expected to be more strongly bound to the substrate than any other partial dissociation product NH_x . This should explain why atomic nitrogen is associated with the lowest BE since the relevant extra-atomic relaxation energy should be highest among all NH_x species ($x=0,1,2,3$) chemisorbed on Si(100). But true chemical shifts can also be invoked. Their rapid increase, when T_S increases between 350 and 600°C for exposures above a few L, could be caused both by the succeeding NH_x and H desorptions now opening up more Si sites for N chemisorption, in contrast to the low- T_S adsorption regime, and by the increase with T_S of the NH_3 complete dissociation rate favoring also more N chemisorption. An Arrhenius plot [Fig. 6(a)] for the adsorption at 200 L on *c*-Si(100) surface leads to an apparent activation energy value $E_A \sim 0.19$ eV, in agreement with reported dissociation barrier energies for NH_3 .¹⁷ Other authors arrived at similar conclusions^{18,19} in studying the PH_3 chemisorption on Si. Thus the rapid onset near 400°C obtained by Yu *et al.*¹⁸ for silicon phosphorization by PH_3 similar to ours for nitridation by NH_3 , suggests a mechanism governed more by a common H desorption than by the dissimilar Si—P and Si—N bond strengths.

Useful information about the local Si environments may be derived from the observation of the Si 2*p* line (Figs. 7 and 8). Neither by adsorption on *c*-Si surfaces (Fig. 7), nor by film growth (Fig. 8) could we observe, at 500°C , for example, the well-known shift (of 2.7 eV) of the Si 2*p* line in the nitride environment Si-N₄ as is observed at higher T_S (800°C). Even if the nitrogen atoms are in their nitride environment N-Si₃, they are not numerous enough and the bulk diffusion is too weak to satisfy the nitride local order for Si (Si-N₄). Thus subnitride environments are formed by adsorption as well as during film growth in these conditions. But they do not correspond to an equally weighted distribution of the statistically possible tetrahedral Si-(Si_{4-x}N_x) $x=0,1,2,3,4$. Owing to the systematic shoulder at ~ 2 eV from the

pure Si-Si₄ signal, a preponderant Si-SiN₃ form must be suggested, particularly for surface adsorption. Such views are compatible with Si top-layer atoms threefold laterally bonded to nitrogen atoms and back bonded with Si atoms in agreement with some models, as deduced by EELS,²⁰ for nitridation of Si(111) surfaces with N atoms. The situation seems to be more complicated in amorphous films presenting more varying environments (Si-Si₂N₂).

As a function of exposure (Fig. 9) the nitridation in this 500 – 600°C region rises rather rapidly at low exposure but the further increase above coverage values, increasing with T_S , comprised between 1 and 2×10^{15} atoms cm^{-2} is very smooth. These values are higher than the RT saturation coverage ($\sim 2 \times 10^{14}$ atoms cm^{-2}), but nevertheless prove that the nitridation remains limited, in this T_S range, in the vicinity of the top layer by deficient bulk diffusion. However, it is important to note that no low

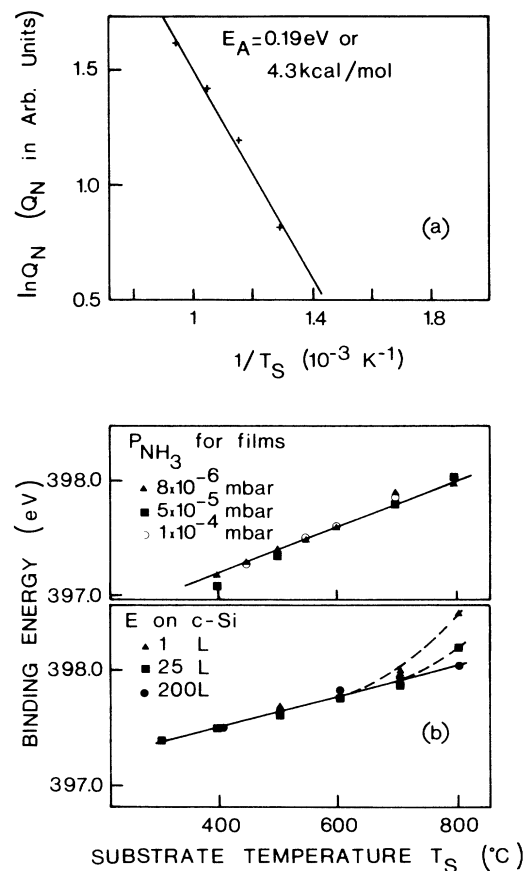


FIG. 6. (a) Arrhenius plot of the nitrogen uptake Q_N on *c*-Si(100)- 2×1 surfaces exposed to 200 L ($t=133$ sec, $p=2 \times 10^{-8}$ mbar) of NH_3 . (b) Similar BE changes with T_S for the N 1*s* core levels in deposited films (upper curve) or upon *c*-Si surfaces (lower curve) when deposited under, or exposed to, respectively, various NH_3 pressures. Note in the latter case only, the BE shift at the lowest exposures near 800°C , attributed to the low- T_S readsorption of NH_x fragments on the unoccupied Si surfaces states after the high- T_S exposure.

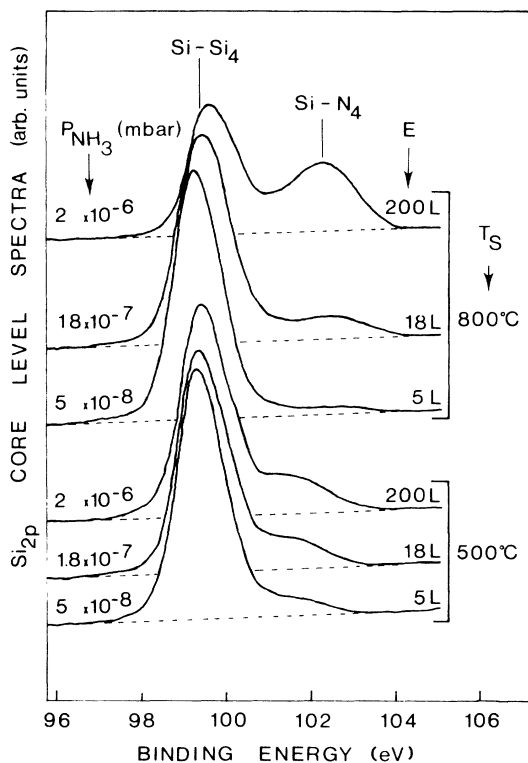


FIG. 7. Si 2p core-level lines illustrating the Si local environment changes with T_S after nitrogen adsorption upon c -Si(100)- 2×1 surfaces.

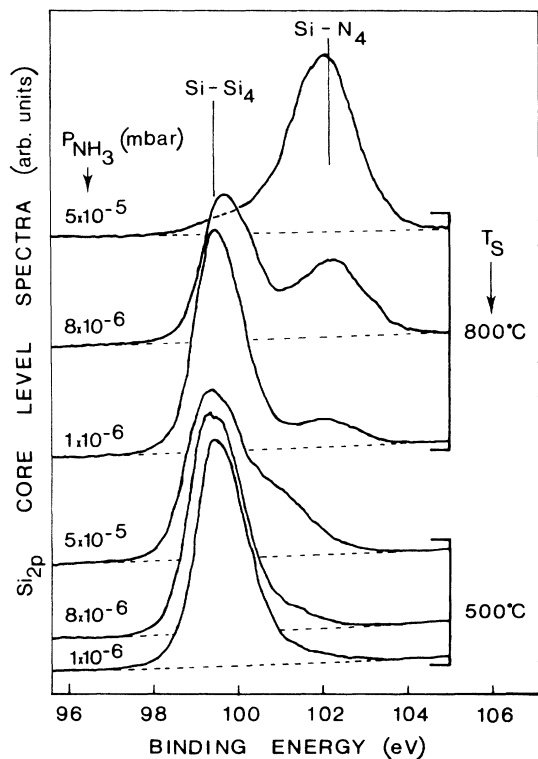


FIG. 8. Si 2p core-level lines illustrating the Si local environment changes with T_S in the nitride films deposited under an NH_3 ambient.

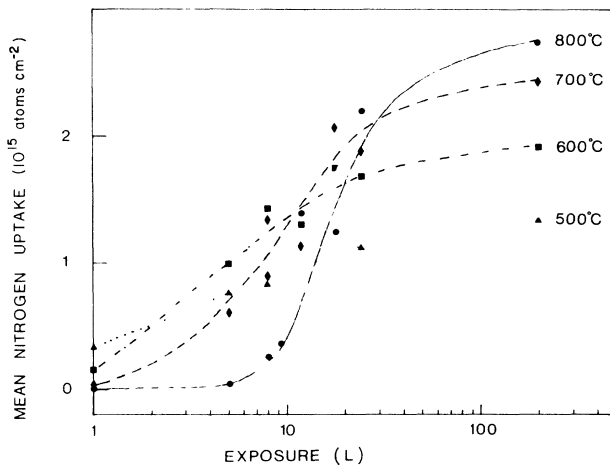


FIG. 9. XPS nitrogen uptake upon c -Si(100)- 2×1 surfaces as a function of the NH_3 exposure (constant time $t=133$ sec, varying pressure) for various T_S .

T_S surface readorption of NH_x species could be observed after such nitridation followed by post RT NH_3 exposure. This suggests a nearly spatially uniform N chemisorption capping all Si surface dangling bonds in a randomly distributed way. Such statements are in accordance with the angular dependence of the N 1s signal in favor of a localization of the nitrogen atoms mainly limited to the top layer in this stage.

We end finally with the highest- T_S domain studied ($600 < T_S < 800^\circ\text{C}$). The most prevailing feature is an enhanced phase separation as illustrated at 800°C by the Si 2p line behavior on c -Si surfaces (Fig. 7), and the film growth (Fig. 8). Even for the lowest-used pressure for which the nitridation is very weak, only large shifts (i.e., 2.7 eV as in bulk nitride) (Refs. 21 and 22) in the BE's could be observed, providing evidence for the presence of true nitride local environments (Si-N_4 and N-Si_3). This thermodynamically more favorable phase separation is further favored by an enhanced nitrogen diffusion and penetration into the substrate. The presence of such bonds, at very low coverage on c -Si surfaces, evidently precludes a uniform top layer growth and requires tridimensional growth as will be shown below.

The SiN_x deposits prepared under the above conditions of T_S and dynamical exposure are clearly heterogeneous (mixtures of Si and Si_3N_4) (Fig. 8) as already emphasized in a previous report²² dealing with the ion-bombardment smoothing of such heterostructures. The clustering of Si-Si_4 and Si-N_4 units becomes more complete as T_S increases. Indeed, at lower T_S , more intermediate $\text{Si}(\text{Si}_{4-x}\text{N}_x)$, $x=2$ and 3 connecting the previous phases, are formed, leading to a smoothing of the Si 2p line and a lowering of the chemical shifts as compared to those reported for pure Si and Si_3N_4 phases.^{21,22}

Comparing now the quantitative nitrogen uptake on c -Si(100) surfaces (Fig. 2) or during film growth (Fig. 3) in the highest- T_S domain, the results can be classified in two pressure or exposure regions.

a. Low pressure or exposure (E or $E_D < 20$ L). The initial increase of the nitridation observed in the intermediate T_S range (350–600°C) is now slowed down in film deposition (Fig. 3) and even completely suppressed for *c*-Si surface adsorption (Fig. 2). In the latter case the nitrogen uptake presents a maximum for T_S values which become higher as the exposure increases. For instance, maxima at 500 and 800°C would correspond to exposures of 1 and 25 L, respectively. This shows the very late but rapid increase of the nitrogen uptake as a function of exposure at high T_S compared to the more pronounced but saturating one at low E and T_S , as illustrated in Fig. 9. It is noteworthy that the same exposure dependence was also found for oxidation.^{23,24} In Fig. 2, on the high- T_S side of these maxima, for low-pressure curves, we also indicate, by dash-marked areas, the deconvoluted contributing part to the N 1s signal of the now well-known low- T_S NH_x readsorption contribution at higher BE (line γ). This contribution is the unavoidable result of the limited pumping speed, and consequently, of the highly reactive RT adsorption process on the bare Si surface and its unquenched surface states, when we return at RT after a high- T_S exposure. This is particularly clear in Fig. 4 for the N 1s peak after 1 L exposure at 800°C where the nitride contribution (line β) to the N 1s peak is nearly negligible. The unique contribution in this case is given by the line γ as for exposure at RT.

But the most interesting feature is obtained by higher exposures (8–20 L) for which the true nitridation is now notably higher [$(\sim 1-2) \times 10^{15}$ atoms cm^{-2}], although the N 1s BE shift and linewidth broadening still characterize the presence of NH_x readsorption [dashed lines at high T_S in Figs. 2 or 6(b)]. This association of relatively high-concentration levels of chemisorbed nitrogen in a silicon nitride configuration (as shown in Fig. 7) together with unquenched surface states after the high- T_S exposure proves undoubtedly the occurrence, at high- T_S , of a heterogeneous Si surface with tridimensional growth of Si_3N_4 islands together with unreacted regions. This nonuniform growth is in agreement with the conclusions of Delord *et al.*²⁵ deduced from LEED observations. Other arguments can be given in order to corroborate this statement.

(i) For similar nitrogen coverage ($\sim 10^{15}$ atoms cm^{-2}) on the low- T_S side of the maximum, no convolution of the hydronitride (Si-NH_x) component can be observed in the N 1s signal besides the nitride N- Si_3 one. On account of the poorer nitrogen mobility in this lower- T_S range only weak segregation would be possible and the coverage would consist in a more uniform nitrogen top-site layer with few unreacted regions.

(ii) An angular study versus T_S of the $I(\text{N } 1s) (\theta=0^\circ)/I(\text{N } 1s) (\theta=60^\circ)$ or $I(\text{Si } 2p) (\theta=0^\circ)/I(\text{Si } 2p) (\theta=60^\circ)$ ratios, for similar N uptakes, allows to ascertain a deeper repartition of the nitrogen atoms when T_S increases. Thus an estimation of nearly 10–12 Å (~ 3 nitride planes) can be proposed for the real island thickness at high T_S (800°C). Besides, examinations of the same ratios at 800°C, as a function of the coverage, reveal nitrogen intensity ratios nearly constant, whatever the cov-

erage in this initial stage, in opposition to the substrate Si signal which is only rapidly attenuated for the highest exposures. Such a behavior can only be explained by a *surface extension variation of the Si_3N_4 islands* with the coverage and not by a *progressive thickness variation* of a uniform nitride overlayer. Therefore the thickness values given in Fig. 2 in this high- T_S domain have to be only understood as indicative mean nitride thicknesses deduced from the simple homogeneous overlayer model. The relationship between the mean nitrogen uptake expressed in atoms cm^{-2} and the thickness d is not unique; in the case of an inhomogeneous overlayer, the real repartition implies a thicker indepth repartition, in an island fashion, instead of a thinner uniform surface layer.

(iii) A careful N 1s BE examination versus T_S [Fig. 6(b)] provides further arguments for the previous model and comforts the similarities between the surface and film-growth adsorption process. Independently from the N 1s BE changes associated with the passage from the NH_x (low- T_S regime) species to the nitride configurations N- Si_3 , another systematic shift could be observed inside the high- T_S domain where only nitride environments interfere. As T_S increases from 400 to 800°C, in the deposited SiN_x films as well as for adsorption on the *c*-Si surface, the N 1s BE in the nitride configuration shifts from the 397.2–397.4 eV range to the 398.0–398.1 eV one [Fig. 6(b)]. This BE change can be well understood considering the previously suggested evolution for nitrogen from subnitride films or top sites (400–600°C) to the local configuration in the nitride islands (600–800°C). In both cases the first neighbors of nitrogen can be supposed the same (three Si atoms) but the Si second neighbors in the semiconducting matrix at the lower T_S are progressively replaced by nitrogen atoms in Si_3N_4 islands or in an insulating matrix at higher T_S . The similarity between the N 1s BE values (398.0–398.1 eV) in bulk Si_3N_4 given by Karcher *et al.*²⁶ with those obtained by us at high T_S for very low mean coverage ($\sim 10^{15}$ atoms cm^{-2}) on the *c*-Si(100) surface supports our hypothesis of initial nitride island growth. These various BE values for N 1s in the nitride configuration may explain some discrepancies in the reported results and possible neglect of, or confusion with, the low- T_S γ line.

The last point that we would like to discuss concerns the quantitatively weak nitrogen uptake in the nonuniform-growth stage at high T_S and low exposure. It slows down by raising T_S for film deposition (Fig. 3) and decreases rapidly for *c*-Si(100) surface adsorption (Fig. 2). In this domain the nitridation rate is no longer determined by the complete NH_3 dissociation rate, which increases with T_S , but by a rising desorption rate of the chemisorbed nitrogen atoms. It has long been established that nitrogen tends to desorb at very high T_S ($T_S > 1000^\circ\text{C}$), probably in the Si_2N form.^{1,27} Our results demonstrate that the temperature for which the desorption rate prevails over the adsorption rate is exposure dependent and can be as low as 500°C for exposures of 1 L. Indeed, for weak pressures the probability for the chemisorbed N atom to react in an island fashion before desorbing should be low, the islands being very distant

from each other. This assumption is confirmed by a slower nitrogen-uptake increase when the exposure time is raised, compared to the effect of a NH_3 pressure increase in the same ratio. The consequences of pressure variations therefore dominate the kinetic factors in this low-exposure or initial-nitridation stage.

b. High pressures or $E > 25$ L. The T_S domain for which the desorption prevails falls above 800°C . For instance, at 800°C , the surface mobility of the nitrogen atoms sufficiently near the now more numerous islands, allows reaction in the nitride form before the desorption. The nitride islands in this exposure range probably coalesce more rapidly and form a nearly uniform nitride overlayer whose further growth will be the focus of part B ($E > 200$ L) of this report. It should be noted that authors arguing in favor of,¹ or admitting² the layer-by-layer growth mode, use a combination of exposure times and pressures higher than ours, and therefore have studied the more uniform-growth regime.

During the film deposition, the desorption process must be somewhat less significant (Fig. 4) at low exposure ($E_D \sim 1$ L), possibly due to the arrival of Si atoms from the gas phase. However, we also notice that even if the exposure ranges are comparable during film growth and surface adsorption, because of experimental evaporation constraints, the exposure times are nearly 100 times lower in film growth ($t_D \sim 1$ sec) and the pressures 100 times higher compared to the surface adsorption. For dynamical exposure values of $E_D \sim 200$ L the nitride Si_3N_4 stoichiometry is almost reached at 800°C , and nitrogen incorporation is saturated, all Si coordination sites being occupied by nitrogen.

At this stage of the study a more general comparison with the extensively studied oxidation process can be conducted in order to generalize to the nitridation some concepts found for oxidation. Thus, if we discard a T_S shift accounting for the RT dissociative oxygen chemisorption, the nitrogen one only starts above 350°C (after the low- T_S NH_x and H chemisorption regimes), and the curves shown in Fig. 2 or the exposure dependence in Fig. 9 will be very similar to the one obtained by Tabe²⁴ for initial oxidation. In both cases strongly T_S -dependent behaviors are found. In the lowest- T_S range (RT for oxidation, 350 – 600°C for nitridation) fast adsorption stages ending at low exposures (~ 40 L) and characterized by the presence of many undercoordinated Si sites (suboxides, subnitrides) are obtained. On the basis of two O 1s components Hollinger *et al.*²⁸ differentiated top and bridge sites at the overlayer and near it, respectively. At high T_S , temperature-induced phase separation is a well-known bulk property of SiO_x films.^{29,30} More recently the presence of microcrystallized SiO_2 islands was detected by high-resolution electron microscopy for the earlier growth of silicon oxide on Si.³¹ Our report is the first to reveal such similarities in the T_S -dependent behavior of the silicon nitridation and oxidation. Thus, the nitrogen-uptake decrease observed by us at high T_S and low exposure in the island growth mode, and interpreted as due to strong nitrogen desorption (Si_2N form²⁷), can be matched well with the similar oxygen-uptake decrease,

attributed to oxygen desorption (in the SiO form³²). It explains why high- T_S treatment produces passivating SiO_2 or Si_3N_4 layers with high pressures or exposures while it is a usual surface cleaning procedure at low pressure. As emphasized by Tabe *et al.*²⁴ for oxidation, we also find for nitridation an increasing transition pressure or exposure for each increasing T_S , separating the "passivation" mode of the nitride from the "combustion" one (Fig. 2).

B. The slow-nitridation stage

We present now more detailed data concerning the slowing down stage following the rapid initial nitridation at high T_S (700 – 800°C) and high pressure or exposure ($E > 200$ L) (Fig. 1). The exposures used are now high enough for the assumption of homogeneous growth to be verified. Moreover this section only addresses the question of thermal nitridation of $\text{Si}(100)$ - 2×1 surfaces and not of film deposition since complete nitridation in Si_3N_4 is already achieved at these T_S for dynamical exposures in the vicinity of $E_D \sim 200$ L (Fig. 3). As was shown in Fig. 1 or by other authors,^{1,2} in contrast with the oxidation slow stage, the nitridation can be characterized by a more marked slowing down and its growth nearly stops. These processes are now well known to be limited by the transport mechanism of the reacting species through the film already formed; the better diffusion-barrier properties for the nitride account for this difference. Our aim in this section is to explore the until-now undetermined laws governing the high- T_S nitridation rate, i.e., its pressure dependence (at constant time) and its time dependence (at

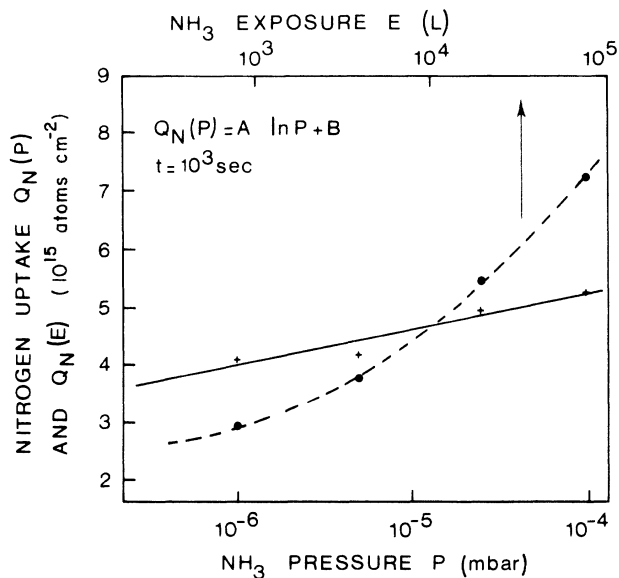


FIG. 10. Nitrogen uptake on $c\text{-Si}(100)$ - 2×1 at 700°C : +, constant exposure time (10^3 sec) as a logarithmic function of pressure P (lower scale) or exposure (upper scale) [$Q_N(P)$]; • constant pressure (10^{-5} mbar) and rising exposure times [$Q_N(t)$]. The latter curve can only be read with the upper exposure scale.

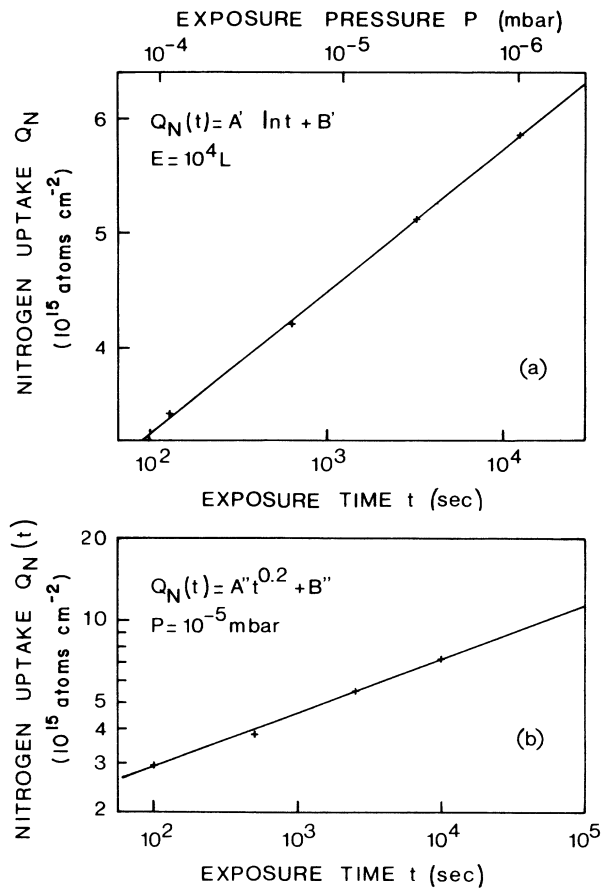


FIG. 11. (a) Nitrogen uptake on $c\text{-Si}(100)\text{-}2 \times 1$ at 700°C at constant exposure ($E = 10^4 \text{ L}$) vs logarithm of increasing exposure times or decreasing exposure pressures. (b) $\ln\text{-}\ln$ representation of the nitrogen uptake $Q_N(t)$ vs exposure time at $T_S = 700^\circ\text{C}$ and $P(\text{NH}_3) = 10^{-5} \text{ mbar}$.

constant pressure) compared to that at constant exposure.

In Fig. 10 the plot of the nitrogen uptake Q_N as a function of the NH_3 pressure or exposure for constant exposure times (10^3 sec) at 700°C indicates a logarithmic law $Q_N(P) = 2.7 \times 10^{14} \ln P + B$ with P in mbar and Q_N in

atoms cm^{-2} . We derive

$$\left. \frac{dQ}{dP} \right|_{t, T_S} \sim \frac{1}{P} \quad \text{or} \quad \left. \frac{dQ}{dP} \right|_{10^3 \text{ sec}, 700^\circ\text{C}} \sim \exp(-\alpha Q).$$

The comparison with the second curve in Fig. 10 (which corresponds only to the exposure scale) visualizes that a faster-nitridation rate is obtained if the same exposure variations originate from a time variation instead of a pressure one. We immediately conclude that pressure and time are not involved in the same way in the exposures of the high- T_S nitridation. This statement can be further illustrated in Fig. 11(a). Increasing nitrogen uptakes are obtained when working at constant exposures, with exposure time increasing when balanced by pressure decrease. A better way to increase nitridation is therefore to increase rather the nitridation time than the pressure. Indeed, in this slow stage, in contrast with the initial nitridation stage for which preponderant pressure variations were found (Sec. III A), the reaction is weakly pressure dependent ($Q_N \sim \ln P$) and time dependence in the exposure leads to more prevailing variations for Q_N ($\sim t^{0.2}$) [Figs. 10 and 11(b)].

These results suggest several comments. The exposure E alone, i.e., only expressed in Langmuirs, without pressure or time dependence, cannot be a good parameter for the description of the nitridation process, despite its use of numerous surface studies. The pressure dependence of the nitrogen uptake in terms of a logarithmic law, found by us for pressures comprised between 10^{-6} and 10^{-4} mbar, seems to be valid in a much larger pressure range. Indeed, in an earlier report,³³ concerning NH_3 nitridation at atmospheric pressure, Hayafuji and Kajiwara also obtained a logarithmic law. The extrapolation of our empirical pressure law to the high pressures leads to nitride thicknesses compatible with those reported by these authors.

All relationships between the nitridation rates at $T_S = 700^\circ\text{C}$ and time t , pressure P , or exposure E deduced from the curves in Figs. 10 and 11 are summarized in Table I.

These relations account for the decreasing nitridation rates, when the layer thickness increases. The decrease is more rapid when caused by pressure variations (exponen-

TABLE I. Empirical laws deduced from Figs. 10 and 11.

Constant time $t = 10^3 \text{ sec}$ $T_S = 700^\circ\text{C}$	Constant exposure $E = 10^4 \text{ L}$ $T_S = 700^\circ\text{C}$	Constant pressure $P = 10^{-5} \text{ mbar}$ $T_S = 700^\circ\text{C}$
$Q_N(P) = A \ln P + B$	$Q_N(t) = A' \ln t + B'$	$Q_N(t) = A'' t^{0.2} + B''$
$\left. \frac{dQ}{dP} \right _{t, T_S} = \frac{A}{P}$	$\left. \frac{dQ}{dt} \right _{E, T_S} = \frac{A'}{t}$	$\left. \frac{dQ}{dt} \right _{P, T_S} = \frac{0.2 A''}{t^{0.8}}$
$\left. \frac{dQ}{dP} \right _{t, T_S} \sim \exp^{-Q/A}$	$\left. \frac{dQ}{dt} \right _{E, T_S} \sim \exp^{-Q/A'}$	$\left. \frac{dQ}{dt} \right _{P, T_S} \sim \frac{1}{(Q - B'')^4}$
$A \sim 2.7 \times 10^{14} \text{ atoms/cm}^2$ impinging molecules $\sim P$	$A' \sim 5.4 \times 10^{14} \text{ atoms/cm}^2$ impinging molecules $\sim \text{constant}$	$A'' \sim 1.2 \times 10^{15} \text{ atoms/cm}^2$ impinging molecules $\sim t$

tial decrease with the layer thickness) than by time variations (power law) in the exposure E . These results prove the occurrence of a time-dependent process, such as the diffusion of some species, sometimes leaving free Si bonds at the nitride-gas interface. In addition to the number of impinging NH_3 molecules, which depends similarly on pressure and time increases, this diffusion process gives the time variations a second reason to increase the nitridation rate. Diffusion of atomic silicon or nitrogen vacancies across the nitride layer have been suggested.^{33,3} However, since the exact nature of the diffusing species is not yet well known, modeling of our empirical laws would be very risky.

IV. CONCLUSION

All observed correlations on the NH_3 -Si system between film-growth features (T_5 and pressure dependence of the incorporated species, bulk phase segregation, local environments, etc.) and fundamental surface studies (molecular dissociation on electronic surface states, adsorption and dissociation regimes, diffusion of the adsorbed species, etc.) contribute to the conclusion that surface data are very helpful for a better understanding of the film growth. Moreover, some of these results present a general interest because of their common nature with the O_2 -Si system.

-
- ¹A. Glachant and D. Saidi, *J. Vac. Sci. Technol. B* **3**, 985 (1985).
²C. Maillot, H. Roulet, and G. Dufour, *J. Vac. Sci. Technol. B* **2**, 316 (1984).
³C. Maillot, H. Roulet, G. Dufour, F. Rochet, and S. Rigo, *Appl. Surf. Sci.* **26**, 326 (1986).
⁴R. Heckingbottom and P. R. Wood, *Surf. Sci.* **36**, 594 (1973).
⁵S. Tanaka, M. Onchi, and M. Nishijima, *Surf. Sci.* **191**, L576 (1987).
⁶D. G. Kilday, G. Margaritondo, D. J. Frankel, J. Anderson, and G. J. Lapeyre, *Phys. Rev. B* **35**, 9364 (1987).
⁷T. Isu and K. Fujiwara, *Solid State Commun.* **42**, 447 (1982).
⁸R. J. Hamers, P. Avouris, and F. Bozso, *Phys. Rev. Lett.* **59**, 2071 (1987).
⁹L. Kubler, R. Haug, J. J. Koulmann, D. Bolmont, E. K. Hlil, and A. Jaegle, *J. Non-Cryst. Solids* **77/78**, 945 (1985).
¹⁰L. Kubler, E. K. Hlil, D. Bolmont, and J. C. Peruchetti, *Thin Solid Films* **149**, 385 (1987).
¹¹L. Kubler, E. K. Hlil, D. Bolmont, and G. Gewinner, *Surf. Sci.* **183**, 503 (1987).
¹²E. K. Hlil, L. Kubler, J. L. Bischoff, and D. Bolmont, *Phys. Rev. B* **35**, 5913 (1987).
¹³F. Bozso and P. Avouris, *Phys. Rev. B* **38**, 3943 (1988).
¹⁴J. A. Wurzbach, F. J. Grunthaler, and J. Maserjian, *J. Vac. Sci. Technol.* **20**, 962 (1982).
¹⁵R. Flitsch and S. Raider, *J. Vac. Sci. Technol.* **12**, 305 (1975).
¹⁶J. L. Bischoff, L. Kubler, and D. Bolmont, *J. Non-Cryst. Solids* **97/98**, 1407 (1987).
¹⁷S. P. Murarka, C. C. Chang, and A. C. Adams, *J. Electrochem. Soc.* **126**, 996 (1979).
¹⁸M. L. Yu and B. S. Meyerson, *J. Vac. Sci. Technol. A* **2**, 446 (1984).
¹⁹A. J. Van Bommel and F. Meyer, *Surf. Sci.* **8**, 381 (1967).
²⁰K. Edamoto, S. Tanaka, M. Onchi, and M. Nishijima, *Surf. Sci.* **167**, 285 (1986).
²¹S. I. Raider, R. Flitsch, J. A. Aboaf, and W. A. Pliskin, *J. Electrochem. Soc.* **123**, 560 (1976).
²²L. Kubler, R. Haug, E. K. Hlil, D. Bolmont, and G. Gewinner, *J. Vac. Sci. Technol. A* **4**, 2323 (1986).
²³P. Collot, G. Gautherin, B. Agius, S. Rigo, and F. Rochet, *Philos. Mag. B* **52**, 1051 (1985).
²⁴M. Tabe, T. T. Chiang, I. Lindau, and W. E. Spicer, *Phys. Rev. B* **34**, 2706 (1986).
²⁵J. F. Delord, A. G. Schrott, and S. C. Fain, *J. Vac. Sci. Technol.* **17**, 517 (1980).
²⁶R. Karcher, L. Ley, and R. L. Johnson, *Phys. Rev. B* **30**, 1896 (1984).
²⁷A. G. Schrott, Q. X. Su, and S. C. Fain, *Surf. Sci.* **123**, 223 (1982).
²⁸G. Hollinger, J. F. Morar, F. J. Himpsel, G. Hughes, and J. L. Jordan, *Surf. Sci.* **168**, 609 (1986).
²⁹G. Hollinger, Y. Jugnet, and T. M. Duc, *Solid State Commun.* **22**, 277 (1977).
³⁰J. Finster, D. Schulze, and A. Meisel, *Surf. Sci.* **162**, 671 (1985).
³¹F. Rochet, S. Rigo, M. Froment, C. D'Anterrosches, H. Roulet, and G. Dufour, *Philos. Mag. B* **55**, 309 (1987).
³²M. P. D'Evelyn, M. M. Nelson, and T. Engel, *Surf. Sci.* **186**, 75 (1987).
³³Y. Hayafuji and K. Kajiwara, *J. Electrochem. Soc.* **129**, 2102 (1982).